Has Arctic Sea Ice Loss Contributed to Increased Surface Melting of the Greenland Ice Sheet?

JIPING LIU,* ZHIQIANG CHEN,+ JENNIFER FRANCIS,# MIRONG SONG,+ THOMAS MOTE,@ AND YONGYUN HU&

* *Department of Atmospheric and Environmental Sciences, University at Albany, State University of New York, Albany, New York*
+ *State Key Laboratory of Numerical Modeling for Atmospheric Sciences and Geophysical Fluid Dynamics, and Institute of Atmospheric Physics, Chinese Academy of Sciences, Beijing, China*
# *Department of Marine and Coastal Sciences, Rutgers, The State University of New Jersey, New Brunswick, New Jersey*
@ *Department of Geography, University of Georgia, Athens, Georgia*
& *Department of Atmospheric and Oceanic Sciences, School of Physics, Peking University, Beijing, China*

(Manuscript received 3 June 2015, in final form 21 January 2016)

ABSTRACT

In recent decades, the Greenland ice sheet has experienced increased surface melt. However, the underlying cause of this increased surface melting and how it relates to cryospheric changes across the Arctic remain unclear. Here it is shown that an important contributing factor is the decreasing Arctic sea ice. Reduced summer sea ice favors stronger and more frequent occurrences of blocking-high pressure events over Greenland. Blocking highs enhance the transport of warm, moist air over Greenland, which increases downwelling infrared radiation, contributes to increased extreme heat events, and accounts for the majority of the observed warming trends. These findings are supported by analyses of observations and reanalysis data, as well as by independent atmospheric model simulations using a state-of-the-art atmospheric model that is forced by varying only the sea ice conditions. Reduced sea ice conditions in the model favor more extensive Greenland surface melting. The authors find a positive feedback between the variability in the extent of summer Arctic sea ice and melt area of the summer Greenland ice sheet, which affects the Greenland ice sheet mass balance. This linkage may improve the projections of changes in the global sea level and thermohaline circulation.

1. Introduction

The Greenland ice sheet holds a massive amount of frozen water (equivalent to 6–7 m of contemporary sea level rise if it were to melt completely; e.g., Cuffey and Marshall 2000) and is an important modulator of sea level and ocean thermohaline circulation (e.g., Alley et al. 2005; Shepherd et al. 2012; Hu et al. 2011). Recent changes in surface melt of the Greenland ice sheet are well documented (Abdalati and Steffen 2001; Mote 2007; Fettweis et al. 2011; Mernild et al. 2011; Nghiem et al. 2012; Tedesco et al. 2013; Hanna et al. 2013b). Surface melt has increased dramatically since a period of relative stability and modest snow accumulation in the 1970s (Rignot et al. 2008). Larger amounts of surface meltwater have migrated to the ice–bedrock interface, which may be enhancing glacial sliding (Zwally et al. 2002; Shannon et al. 2013), although this effect might be offset by efficient subglacial drainage (Sundal et al. 2011). The ongoing net ice loss due to surface melt and outlet glaciers from Greenland has contributed to ~8 mm of global sea level rise since 1992 (Cuffey and Marshall 2000), contributing about one-third of all land ice melt to rising sea level (Meier et al. 2007). Since 2009, most of the increase in the rate of ice loss has been due to increased surface melt (Enderlin et al. 2014), fueling concerns that sea level rise could accelerate beyond most projections and raise threat levels for coastal communities worldwide. Some explanations have been offered for the increased surface melt, relating to amplified warming in the Arctic that is occurring as a result of a variety of feedbacks (e.g., Serreze and Barry 2011; Pithan and Mauritsen 2014). Darkening of the Greenland ice sheet by impurities in snow increases the absorption of solar radiation,

Corresponding author address: Jiping Liu, Department of Atmospheric and Environmental Sciences, University at Albany, State University of New York, 1400 Washington Ave., Albany, NY 12222.
E-mail: jliu26@albany.edu

DOI: 10.1175/JCLI-D-15-0391.1

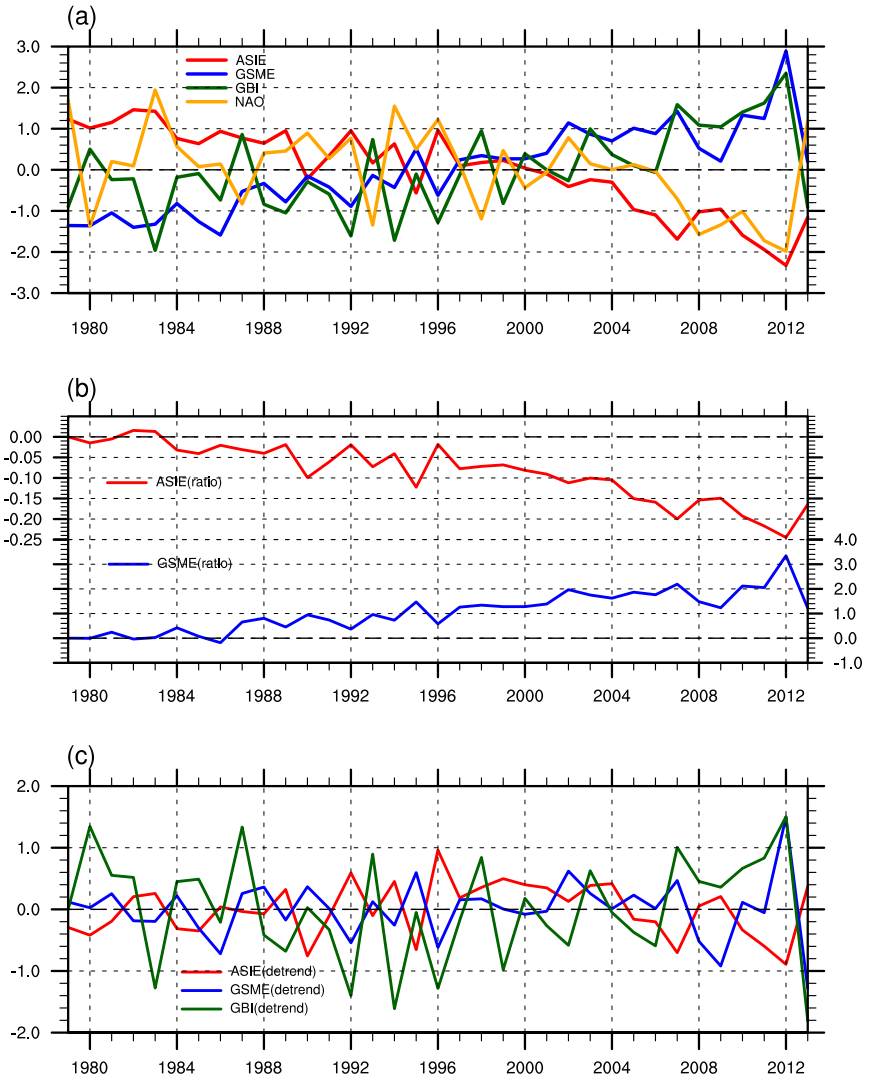

FIG. 1. (a) Temporal variability of summer ASIE, GSME, GBI, and NAO. (b) Percentage change of summer ASIE and Greenland ice sheet surface melt relative to 1979. (c) As in (a), but for detrended indices. Note that all indices are standardized.

enhancing the albedo–melt feedback (Tedesco et al. 2011; Box et al. 2012; Dumont et al. 2014). Temperature variations over Greenland have been linked to the variations of the North Atlantic Oscillation (NAO) (Hanna et al. 2013a). The summer NAO has shown a marked decreasing trend since the mid-1990s (Fig. 1a; e.g., Hanna et al. 2015), which might be related to an anomalous Rossby wave train originating from sea surface temperature (SST) variability in the tropical Pacific (Ding et al. 2014). However, the relationship of year-to-year variability (after removing the linear trend) between SST in the tropical Pacific and surface temperature over most of Greenland is weak and not statistically significant [see extended data Fig. 8b in Ding et al. (2014)]. Hanna et al. (2013a) pointed out that summer temperatures along the Greenland coast and ice sheet runoff are more strongly influenced by blocking patterns over Greenland than by the NAO. In July 2012, for example, approximately 97% of Greenland's ice sheet experienced surface melt, including the summit and dry snow faces of the ice sheet (e.g., Nghiem et al. 2012; Tedesco et al. 2013; Hanna et al. 2014). This extreme melt event was associated with an anomalously persistent ridge of warm air that stagnated over Greenland, along with thin, low-level liquid clouds that modulated the surface energy balance (Bennartz et al. 2013).

Increased ice sheet melt also coincides with a period of rapid decline of Arctic sea ice (Rennermalm et al. 2009), which is both a driver and a consequence of Arctic amplification (e.g., Screen and Simmonds 2010;

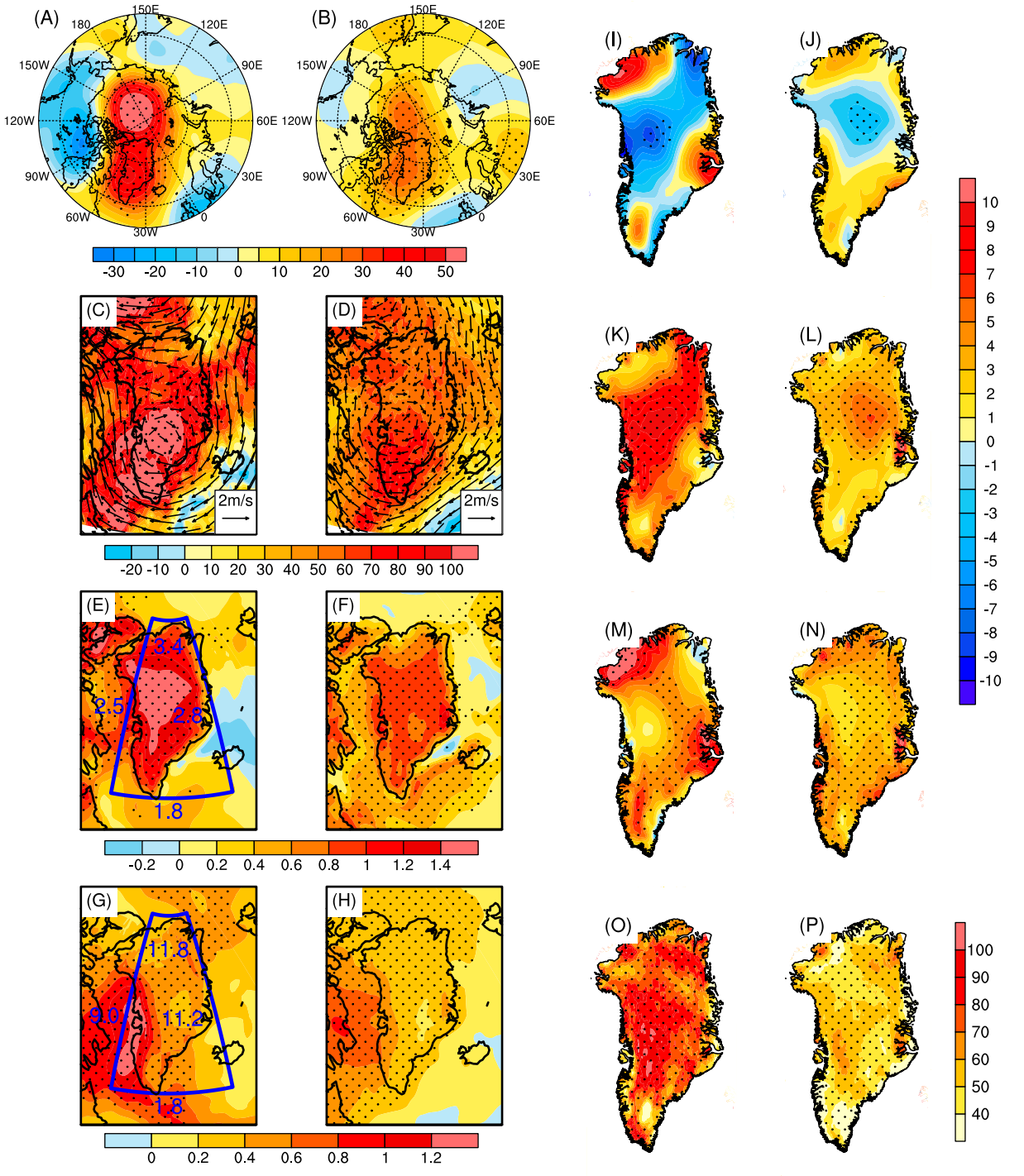

FIG. 2. Summer atmospheric anomalies over Greenland regressed on (first and third columns) detrended and (second and fourth columns) raw (without detrending) summer Arctic sea ice extent index. (a),(b) The 500-hPa geopotential height (m); and (c),(d) 700-hPa wind (vectors; m s^{-1}) and ratio between the number of blocking events based on the regression with ASIE and the summer climatology of blocking events (color shading; %). (e),(f) Surface temperature (color shading; °C) and budget of vertically integrated heat flux from the surface to 300 hPa across horizontal boundaries (blue box; $\times 10^{15}$ W); the values inside (outside) the box denote inflow (outflow) of flux. (g),(h) Vertically integrated specific humidity from surface to 300 hPa (color shading; kg m^{-2}) and budget of water vapor flux across horizontal boundaries (blue box; $\times 10^{6}$ kg s^{-1}). (i),(j) Downward surface shortwave radiative flux (W m^{-2}). (k),(l) Downward surface longwave radiative flux (W m^{-2}). (m),(n) Net downward surface radiative flux (W m^{-2}). (o),(p) Ratio between regressed the number of extreme heat events based on the regression with ASIE and the summer climatology of extreme heat events (%). Grid points that are statistically significant (>95% confidence level) are marked by black dots. Note that the units are with respect to one unit of deviation change in the indices and that the sign of ASIE is reversed.

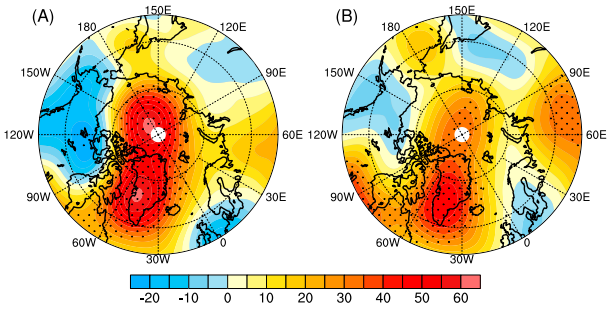

FIG. 3. Summer 200-hPa geopotential height (m) over Greenland regressed onto (a) summer Arctic sea ice extent index and (b) Greenland ice sheet surface melt index. Grid points that are statistically significant (>90% confidence level) are marked by black dots. Note that the sign of ASIE is reversed.

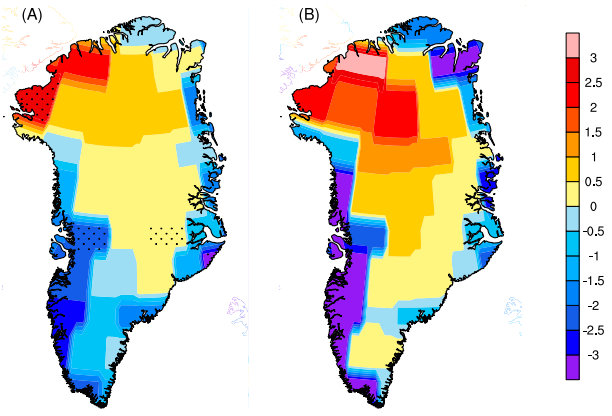

FIG. 4. Summer low-level cloud amount (%) from ISCCP regressed on (a) Arctic sea ice and (b) Greenland surface melt indices (here low-level clouds are defined as cloud-top pressure > 680 hPa). Note that the sign of ASIE is reversed.

Serreze and Barry 2011). However, the potential linkage and mechanisms responsible for the linkage have received relatively little attention. There is a growing body of evidence that a rapid decline in Arctic sea ice is influencing the northern mid- and high-latitude atmospheric circulation (e.g., Francis and Vavrus 2012, 2015; Liu et al. 2012; Cohen et al. 2014; Walsh 2014; Hall et al. 2015; Coumou et al. 2015; Overland et al. 2015). In this study, we find that Arctic sea ice is an important contributor to recent surface melt over Greenland through the effects of sea ice loss on the atmosphere, and we reveal a physical mechanism underlining their connectivity using both observational data and numerical simulations.

2. Data and methods

We use a combination of satellite-derived Arctic sea ice extent and Greenland surface melt extent, the ERA-Interim atmospheric reanalysis, and the Hadley Centre sea surface temperature dataset. We use post-1979 data only because the analyses of atmospheric circulation (e.g., geopotential height) over northern high latitudes are more reliable during the modern satellite era. The common time period for all datasets is from 1979 to 2013. Arctic sea ice extent and concentrations are obtained from the National Snow and Ice Data Center, which are derived from the *Nimbus-7* Scanning Multichannel Microwave Radiometer (SMMR), the DMSP Special Sensor Microwave Imager (SSM/I), and the DMSP Special Sensor Microwave Imager and Sounder (SSMIS) sensors (Comiso 2000; Fetterer et al. 2002). Greenland surface melt extent is generated from gridded brightness temperatures from SMMR, SSM/I, and SSMIS passive microwave radiometers (Mote et al. 1993; Tedesco 2007). The Greenland ice sheet surface melt extent index is defined as the averaged Greenland melt area anomaly divided by its standard deviation. The monthly and daily atmospheric fields are obtained from ERA-Interim (Dee et al. 2011). Sea surface temperature is obtained from the Met Office Hadley Centre (Rayner et al. 2003). Cloud amount is obtained from the International Satellite Cloud Climatology Project (ISCCP), which has revealed its usefulness in the interpretation of cloud properties and evaluation of climate models (e.g., Rossow and Schiffer 1999).

We estimate trends using standard least squares linear regression. We also use regression analysis to identify associations between sea ice variability, Greenland melt area, and atmospheric responses. The statistical significances of the regressions are calculated from a two-tailed t test.

To further assess the robustness of the identified atmospheric fingerprint associated with the reduction of Arctic sea ice using ERA-Interim, we repeat the regression analysis using independent station- and satellite-based datasets. For surface temperature, we use both surface-based observations and satellite retrievals. The surface-based dataset is from the University of Delaware station-based terrestrial temperature (http://climate.geog.udel.edu/~climate/html_pages/Global2011), compiled from a large number of stations [including the Global Historical Climate Network; the Atmospheric Environment Service/Environment Canada; the State Hydrometeorological Institute of St. Petersburg, Russia; the Greenland Climate Network (GC-Net); the Automatic Weather Station Project; the Global Synoptic Climatology Network; and the Global Surface Summary of the Day], which is available for 1979–2010. Satellite retrievals of surface temperature are obtained from the NASA GEWEX Surface Radiation Budget, release 3.0 (SRB 3.0), which is available for 1984–2007 (Stackhouse

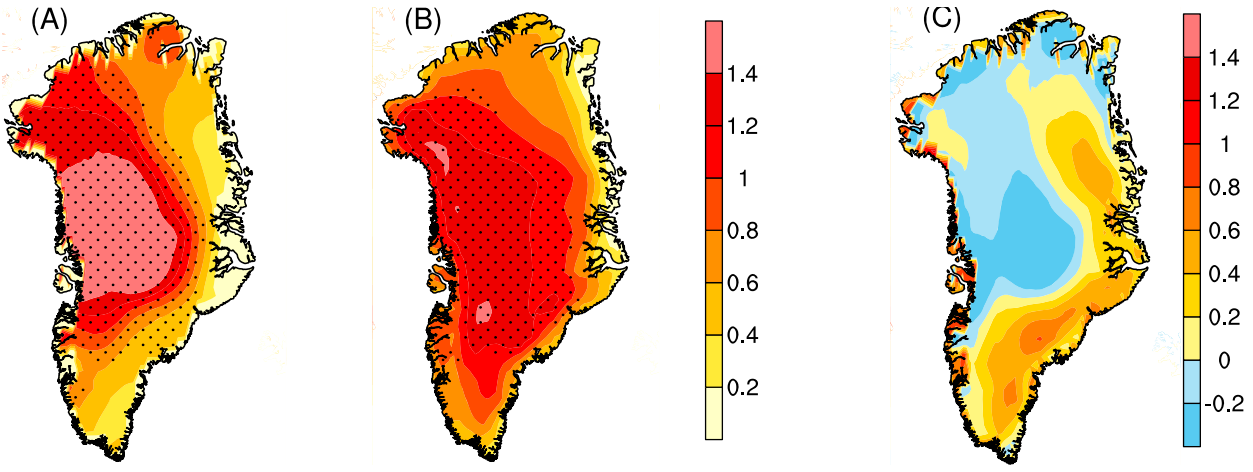

FIG. 5. Summer surface temperature anomalies (°C) over Greenland regressed onto the summer ASIE during 1979–2010. (a) University of Delaware station-based temperature, (b) ERA-Interim, and (c) the difference between (b) and (a). Grid points that are statistically significant (>95% confidence level) are marked by black dots. Note that the sign of ASIE is reversed.

et al. 2011). For surface downwelling longwave radiation, we also use SRB 3.0.

Blocking events are defined as intervals in which daily 500-hPa geopotential height (GPH) anomalies from ERA-Interim exceed 1 standard deviation about the climatological mean for at least five consecutive days (Thompson and Wallace 2001). Extreme heat events are defined as daily maximum surface temperature from ERA-Interim exceeding 1.5 standard deviations above the climatological mean.

Fluxes of heat and water vapor are calculated by determining the total flux crossing the boundary; for example, the vertically integrated meridional component of the water vapor flux across the southern boundary Q_s is calculated as follows:

$$Q_s = -\frac{1}{g}\int_{\lambda_W}^{\lambda_E}\int_{p_s}^{p}(qv)a\cos\phi_s\, d\lambda\,,$$

where q is specific humidity and v is meridional wind. The column extends from the surface p_s to a pressure level p (300 hPa; note that the atmosphere above 300 hPa is dry and contributes little to the water vapor transport process). The quantities λ_E and λ_W are the longitude of the

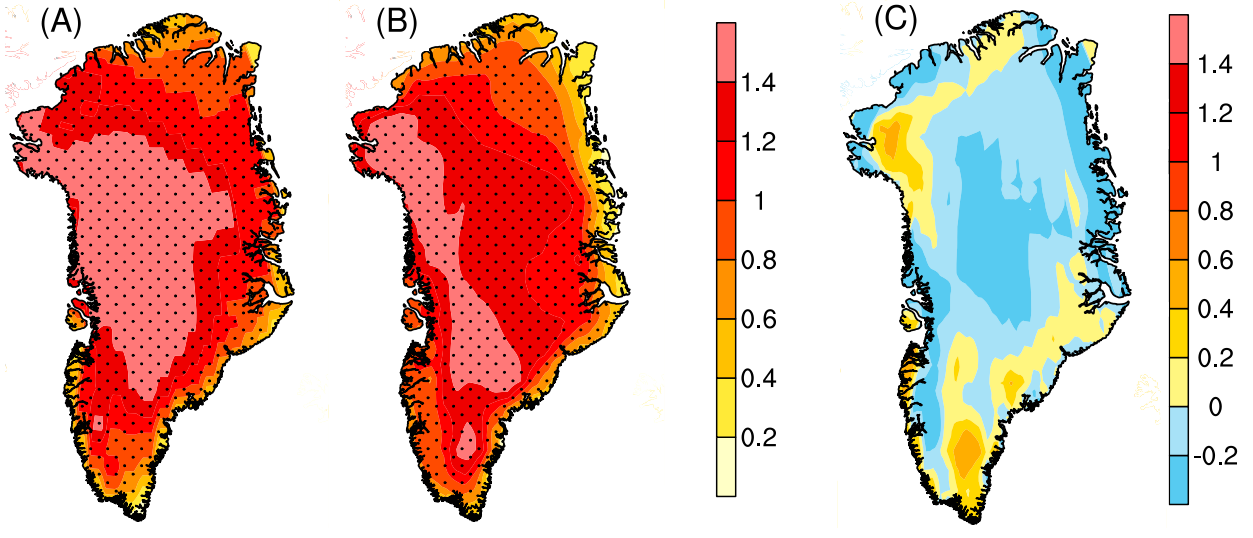

FIG. 6. Summer surface temperature anomalies (°C) over Greenland regressed onto the summer ASIE during 1984–2007. (a) Satellite-based SRB 3.0, (b) ERA-Interim, and (c) the difference between (b) and (a). Grid points that are statistically significant (>95% confidence level) are marked by black dots. Note that the sign of ASIE is reversed.

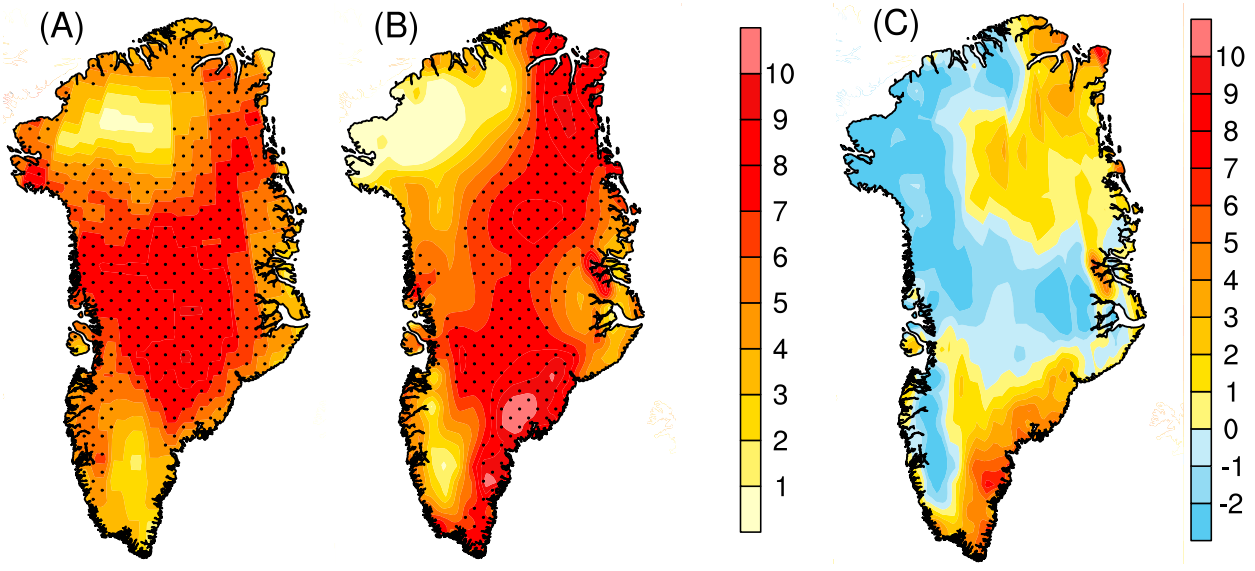

FIG. 7. As in Fig. 6, but for surface longwave radiative flux ($W m^{-2}$).

eastern and western boundaries, respectively, ϕ_s is the latitude of the southern boundary, g is gravitational acceleration, and a is the radius of the earth.

3. Model experiments

Numerical experiments are performed using the National Center for Atmospheric Research (NCAR) Community Atmospheric Model version 3.1 (CAM3.1; Collins et al. 2006) to investigate the atmospheric response (circulation, radiation, and temperature) over Greenland in summer to an imposed reduction in Arctic sea ice consistent with observations.

Two sets of experiments are conducted, the climatological (REF) and low sea ice (PER) simulations. For REF, the model is run with a prescribed seasonal cycle of climatological sea ice concentration (SIC) and SST. For PER, the prescribed sea ice change in summer is based on regression of the satellite-derived summer SIC on the standardized summer Arctic sea ice index during 1979–2013, which is added to the climatological SIC values. In grid boxes and for months where the SIC is absent relative to the REF, the regressed summer SST on the standardized summer Arctic sea ice index is added to climatological SST values; elsewhere, the climatological SST is used. This captures SST changes directly associated with SIC changes but does not include SST changes outside the Arctic sea ice zone. Screen et al. (2014) suggested that a large ensemble size (around 50 members) is desired to address uncertainties due to atmospheric internal variability. Here both REF and PER are run for 50 yr. Because the prescribed boundary conditions repeat annually but the atmospheric initial conditions vary, each year can be considered an independent realization. The large ensemble size (50 ensemble members) better quantifies the forced response of atmospheric circulation to Arctic sea ice loss as well as the unforced internal variability.

We further address the possibility that the atmospheric circulation over Greenland in a specific summer may be primarily driven by the (random) atmospheric state (i.e., the importance of the initial atmospheric state). We perform additional sets of experiments to investigate the role of observed sea ice anomalies for particular summers in influencing atmospheric circulation over Greenland. Let us use the extreme Arctic sea ice loss and surface melt over Greenland in summer 2012 as an example. To obtain an initial atmospheric condition that is close to the observed atmospheric state on 1 June 2012, we integrate the model with the observed boundary conditions (including observed SIC and SST) from 1 September 2011 to 1 June 2012 (AMIP-type simulation). We then conduct the climatology (REF12) and observed sea ice loss (PER12) simulations, which start from the "observed" atmospheric state on 1 June 2012. Each simulation consists of a 3-month integration (from 1 June to 31 August). For REF12, the model is run with a prescribed climatological summer SIC and SST. For PER12, summer SIC is representative of the observed conditions in 2012. Each simulation consists of 30 ensemble members with small perturbations to the initial atmospheric condition on 1 June 2012.

4. Results

a. *Observations and reanalyses*

During the satellite era (1979 onward), Arctic sea ice extent has dwindled in all months. In summer [average

of June, July, and August (JJA)], the Arctic sea ice extent index (ASIE) decreased substantially (22% relative to 1979; red line in Fig. 1). Meanwhile, the summer Greenland ice sheet surface melt extent index (GSME) increased remarkably (237% relative to 1979; blue line in Fig. 1). The two indices are highly negatively correlated ($r = -0.91$). After removing the linear trend, the correlation is still strong ($r = -0.61$, >99% significance), suggesting that the year-to-year variability of the summer Greenland ice sheet surface melt is closely associated with summer Arctic sea ice variability. Note that the correlation results remain the same as time series expanded to summer 2014. Based on the climatology of summer 500-hPa GPH (not shown) and previous studies (e.g., Fang 2004; Hanna et al. 2014), we present a more Greenland-specific measure of atmospheric circulation, the summer Greenland blocking index (GBI), which is calculated as the averaged 500-hPa GPH anomaly over Greenland (60°–80°N, 15°–75°W). The summer GBI exhibits a significant upward trend in recent decades (green line in Fig. 1) and is highly negatively correlated with the summer ASIE ($r = -0.7$). After removing the linear trend, they are still strongly correlated ($r = -0.6$, >99% significance).

Recent studies suggest that an important contributor to the increased surface melt over Greenland's ice sheet arises from changes in atmospheric circulation patterns. The question remains, however, whether the shift in circulation is associated with, and perhaps driven by, the decreasing Arctic sea ice. To address this question, we first regress a variety of summer atmospheric circulation variables onto the ASIE (Fig. 2). Note that caution is required in performing regressions between two variables that have significant trends. It is possible that two variables linked statistically are physically independent in reality. To circumvent this possibility, we focus on regressions using detrended data to identify the atmospheric fingerprint associated with the reduction of sea ice in the Arctic.

The map of summer 500-hPa GPH anomalies regressed onto the detrended summer ASIE shows that anomalously low sea ice cover is associated with substantially higher GPH over Greenland and that the positive height anomalies extend northward over much of the Arctic Ocean (Fig. 2a). These positive anomalies are compensated by negative GPH anomalies in Canada and western Europe. The pattern bears some resemblance to the negative phase of the NAO. The GPH anomaly extends from the surface to the upper troposphere, suggesting an equivalent barotropic response (Fig. 3a). Hence in summer, an anomalously high pressure pattern is evident throughout the troposphere over Greenland in association with reduced Arctic sea ice.

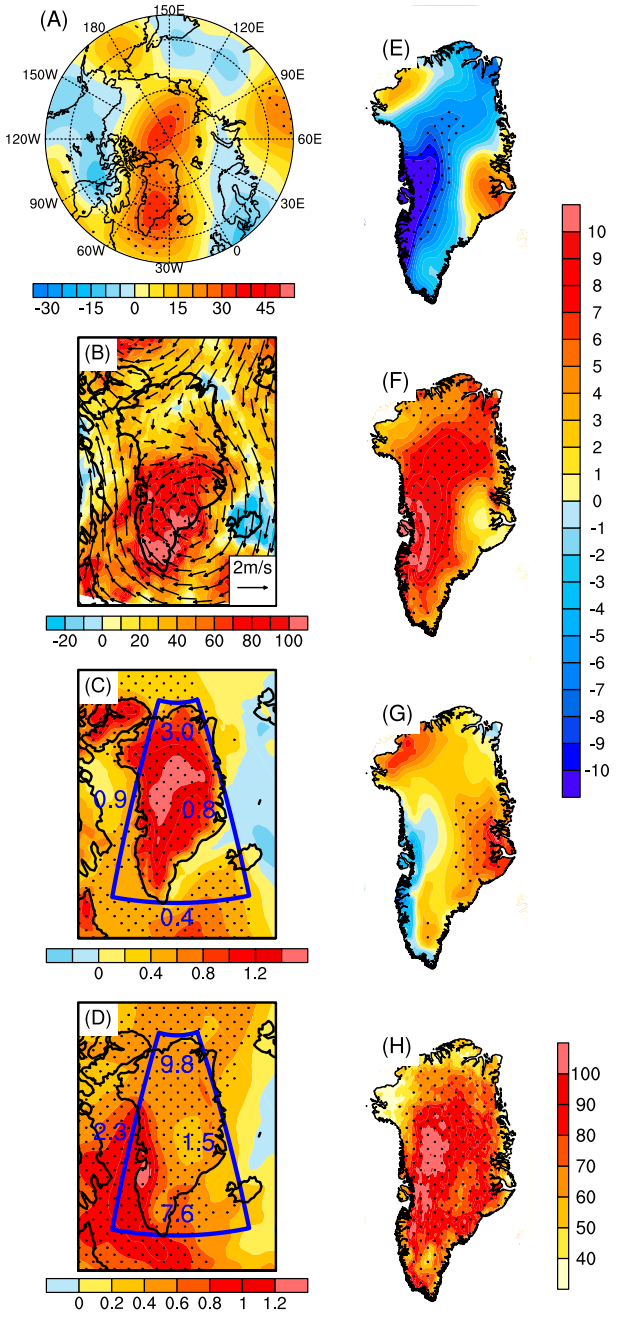

FIG. 8. Summer atmospheric anomalies over Greenland regressed onto Greenland ice sheet surface melt extent index. (a) The 500-hPa geopotential height (m). (b) The 700-hPa wind (vectors; m s^{-1}) and ratio between the number of blocking events based on the regression with the summer GSME and the summer climatology of blocking events (color shading; %). (c) Surface temperature (°C). (d) Vertically integrated specific humidity from surface to 300 hPa (kg m^{-2}). (e) Downward surface shortwave radiation (W m^{-2}). (f) Downward surface longwave radiation (W m^{-2}). (g) Net downward surface radiation (W m^{-2}). (h) Ratio between the number of extreme heat events based on the regression with the summer GSME and the summer climatology of extreme heat events (%). Grid points that are statistically significant (>95% confidence level) are marked by black dots. Note that the units are with respect to one unit of deviation change in the index.

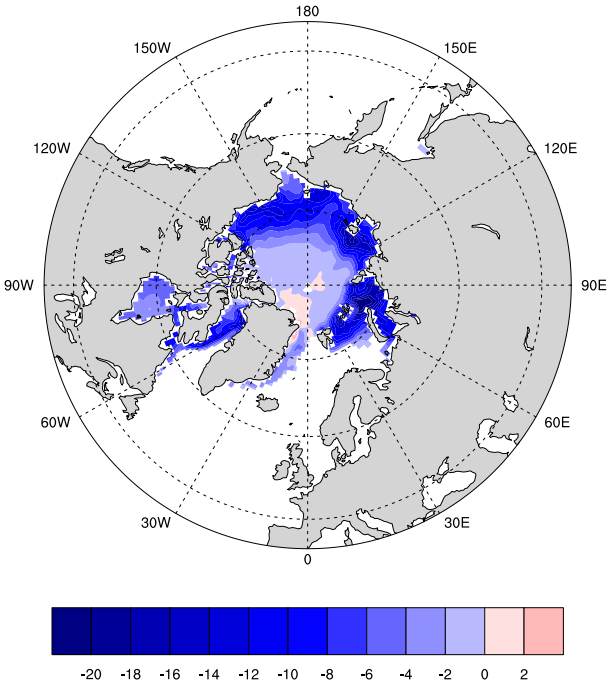

FIG. 9. Prescribed summer sea ice concentration changes in the perturbation model simulation (%).

Figure 2c (color shading) shows the change in summer blocking events over Greenland (see definition in section 2) associated with the reduction in summer Arctic sea ice. An increased incidence of blocking events over Greenland is evident, particularly in central and south Greenland (80%–100% more than the climatological frequency). Hence, in summer, the blocking over Greenland is closely associated with the reduction of Arctic sea ice at both daily and seasonal time scales. As suggested by recent studies (e.g., Hakkinen et al. 2014), blocking over Greenland is linked with the increased area of surface melt across Greenland during recent melt seasons, indicating that Arctic sea ice loss and accelerating Greenland surface melt may also be connected.

An anomalous anticyclonic circulation occupies large parts of central and south Greenland (Fig. 2c, vectors) under the anomalous blocking-high pattern (Fig. 2a), with the largest anomaly over southwest Greenland. Anomalous easterly/northeasterly winds dominate northern Greenland associated with higher GPH in the central Arctic Ocean. Together with the increased frequency of blocking events (Fig. 2c, color) associated with the reduction of Arctic sea ice, these factors lead to a southwestward shift of the climatological high pressure system. The strengthening and southwestward shift of the high pressure system redirects the climatological westerly flows and enhances advection of warm air from the adjacent ocean onto south Greenland. Both favor more frequent incursions of warm and moist air to the Greenland ice sheet from the northwestern Atlantic.

We calculate the vertically integrated heat flux across the horizontal boundaries marked in Fig. 2e. The anomalous circulation pattern associated with the reduction of sea ice leads to heat fluxes across individual boundaries as indicated in Fig. 2e, with a net gain of 2.1×10^{15} W. This additional heat transport enhances the formation of a heat dome over Greenland that promotes additional surface melting (Fig. 2e, color shading). Rennermalm et al. (2009) also found during the melting season a circulation with winds (~270° from north) over southwest Greenland, suggesting that ocean–ice sheet interactions provide favorable conditions for the advection of relatively warm ocean air onto the ice sheet. The dominant flow in all months, however, is northeasterly katabatic wind flowing down the ice sheet interior.

Another potential contributor to the increased surface melt over Greenland's ice sheet arises from increased atmospheric water vapor content linked to the circulation pattern that occurs in association with decreased Arctic sea ice. The regression map of vertically integrated specific humidity shows that in summer, associated with anomalously low ice coverage, total column water vapor increases over all of Greenland and environs, with the largest increase in western and central Greenland (Fig. 2g, color shading), coincident with anomalous southerly wind (Fig. 2c). We also compute the vertically integrated water vapor flux. The reduction of sea ice is associated with a net gain in water vapor transport of 12.2×10^6 kg s^{-1} (Fig. 2g). Increased water vapor content and cloud cover over Greenland reduces the incoming solar radiation while enhancing the downwelling infrared radiation. Associated with sea ice loss, we find reduced insolation extending from western-central to northeastern Greenland (Fig. 2i), corresponding to widespread significant increases in surface downwelling longwave radiation over Greenland (Fig. 2k). Low-level liquid clouds also play an important role in trapping heat near the surface of the ice cap. Associated with the reduction sea ice is an increase in the amount of ISCCP-retrieved low-level liquid clouds (defined as cloud-top pressure >680 hPa) in a large area extending from northwest Greenland into interior high elevations of Greenland (Fig. 4a). Overall, most of Greenland exhibits positive anomalies in surface net downward radiation associated with sea ice reduction (Fig. 2m), indicating the dominance of increasing downward longwave radiation over reduced insolation. This contributes to additional surface heating

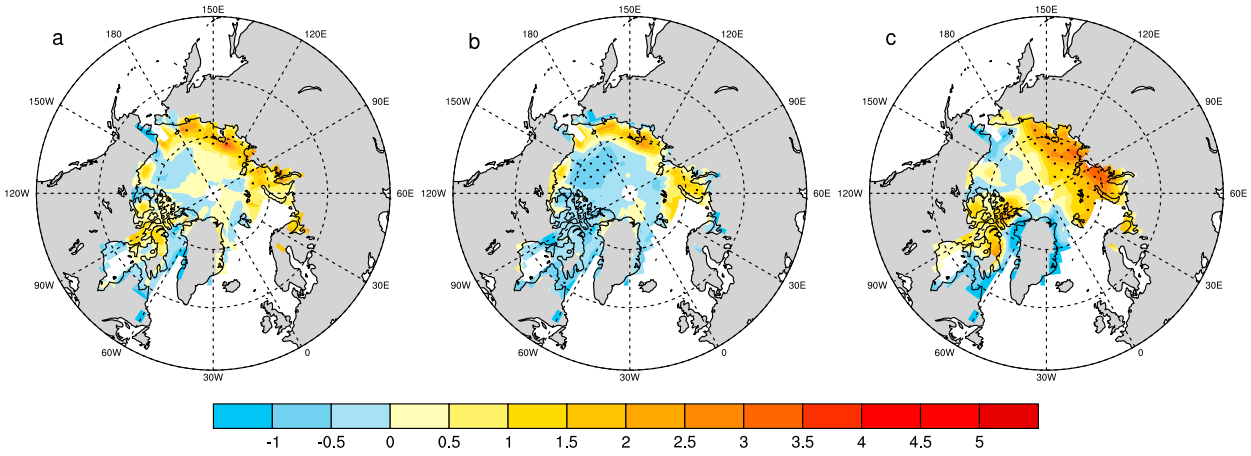

FIG. 10. Response of surface heat flux anomalies (W m^{-2})—(a) sensible heat, (b) latent heat, and (c) net longwave radiation—in summer (positive is from ocean to atmosphere). Grid points that are statistically significant (>95% confidence level) are marked by black dots.

and further albedo reduction through enhanced snow grain metamorphic rates (Box et al. 2012).

We also repeat the regression analysis using the raw data (without detrending; Fig. 2, columns 2 and 4). It appears that variability of the ASIE with trend included is linked to approximately the same patterns of atmospheric circulation, temperature, humidity, and surface radiative flux anomalies as found in year-to-year variability in the detrended ASIE. This provides further confidence that the relationships revealed through regression analyses are physically meaningful.

Figures 5a and 6a present regression maps of detrended station- and satellite-based summer surface temperature anomalies on the detrended summer ASIE. They all show significant warming over Greenland associated with the reduction of Arctic sea ice, which resembles the patterns based on ERA-Interim (Figs. 5b and 6b). Moreover, the map of detrended satellite-based summer downwelling longwave radiation regressed onto the detrended summer ASIE shows widespread significant increases in downward longwave radiation over Greenland (Fig. 7a), which also resembles the reanalysis-based result (Fig. 7b). The consistency between these independent datasets lends confidence to ERA-Interim's surface temperature and downwelling longwave radiation.

The observational analysis described in Fig. 2 indicates that both dynamical (heat transport) and thermodynamic (radiation) effects of decreasing Arctic sea ice are closely associated with atmospheric circulation patterns that appear to contribute to warming (surface melt) over Greenland. We find that the relationship is evident not only in the summer-mean atmospheric temperature (Fig. 2e) but also in increased frequency of extreme heat events over the surface of Greenland (70%–90% more than the climatological frequency of extreme heat events; Fig. 2o).

An indication of a causal relationship is provided by a lagged regression, in which the spatial patterns of detrended summer atmospheric circulation are regressed onto the detrended sea ice extent anomalies averaged over May, June, and July (MJJ), a period one month earlier than the summer average sea ice extent anomalies (JJA). The resulting regression maps are similar to those derived with coincident values (not shown). The similarity of the lagged and simultaneous patterns of atmospheric responses (in both spatial distribution and amplitude) suggests that MJJ sea ice extent anomalies persist into JJA, providing evidence that reduced sea ice may foster circulation patterns that favor warming over Greenland. Markus et al. (2009) showed that Arctic sea ice melt onset has been occurring earlier in recent decades, meaning earlier warming and melting of the sea ice surface, leading to earlier evaporation. The increase of water vapor causes increased cloudiness, which leads to an enhanced greenhouse effect, contributing to increased downward longwave radiation as partly indicated in Figs. 2f,h,l and in agreement with Kapsch et al. (2014).

To further investigate the mechanisms driving the atmospheric responses to the reduction of Arctic sea ice, we repeat the aforementioned regression analysis using the detrended Greenland ice sheet surface melt index. We find that all the atmospheric responses linked to the reduction of summer Arctic sea ice (first and third columns in Fig. 2 and Figs. 3a and 4a) closely resemble those associated with year-to-year variability of the summer GSME, in both spatial distribution and amplitude

(Figs. 8, 3b, and 4b). This lends additional confidence that the associations are robust.

b. *Model simulations*

The real world is very complex, with many aspects of the climate system changing and varying simultaneously. We therefore seek further verification of the associations revealed in our regression analysis of observed fields using targeted model experiments. By forcing an atmospheric model with changes only in sea ice extent, we assess the atmospheric response to that forcing over Greenland to isolate the effects of diminishing sea ice. Two sets of ensemble experiments are conducted using climatological and low sea ice conditions (see section 3 for details). The spatial pattern of prescribed sea ice loss is obtained by regressing observed summer SIC at each grid point onto the summer ASIE during 1979–2013 (Fig. 9), which reflects changes in sea ice cover at each grid point associated with one positive unit of change in the summer ASIE. Thus, the simulated atmospheric circulation change in response to the prescribed sea ice loss can be compared with the aforementioned observation-based regression analysis.

It is well known that variations in the sea ice cover strongly affect surface fluxes of turbulent heat and radiation, both of which affect surface temperature. We calculate the response of the net surface heat flux (the sum of the sensible heat, latent heat, and net longwave radiative fluxes) in the Arctic to the reduction of sea ice. Note that the shortwave radiative flux does not influence the simulation because sea ice and sea surface temperature are specified and are not included in the net heat flux calculation. Significant positive net heat flux anomalies (from the ocean to the atmosphere) are found in the East Siberian, Laptev, Kara, and Barents Seas (where sea ice loss and variability are largest; Fig. 10), which are due almost equally to the surface sensible and latent heat flux and to the net longwave radiative flux anomalies. Thus, the atmosphere exhibits a local thermal response to the reduced sea ice.

The model simulations indicate that heat flux differences owing to the reduced summer Arctic sea ice induce strong positive 500-hPa GPH anomalies over Greenland in summer (Fig. 11a), similar to those revealed by regression using observational data (Fig. 2a). The simulated GPH anomaly configuration drives a flow that enhances the advection of heat and moisture over Greenland (Figs. 11b–d), resulting in increasing downward longwave and net radiation (Figs. 11f,g), widespread warming, and an increased frequency of extreme heat events (Fig. 11h). The consistency between model simulations and observations supports the hypothesized linkage.

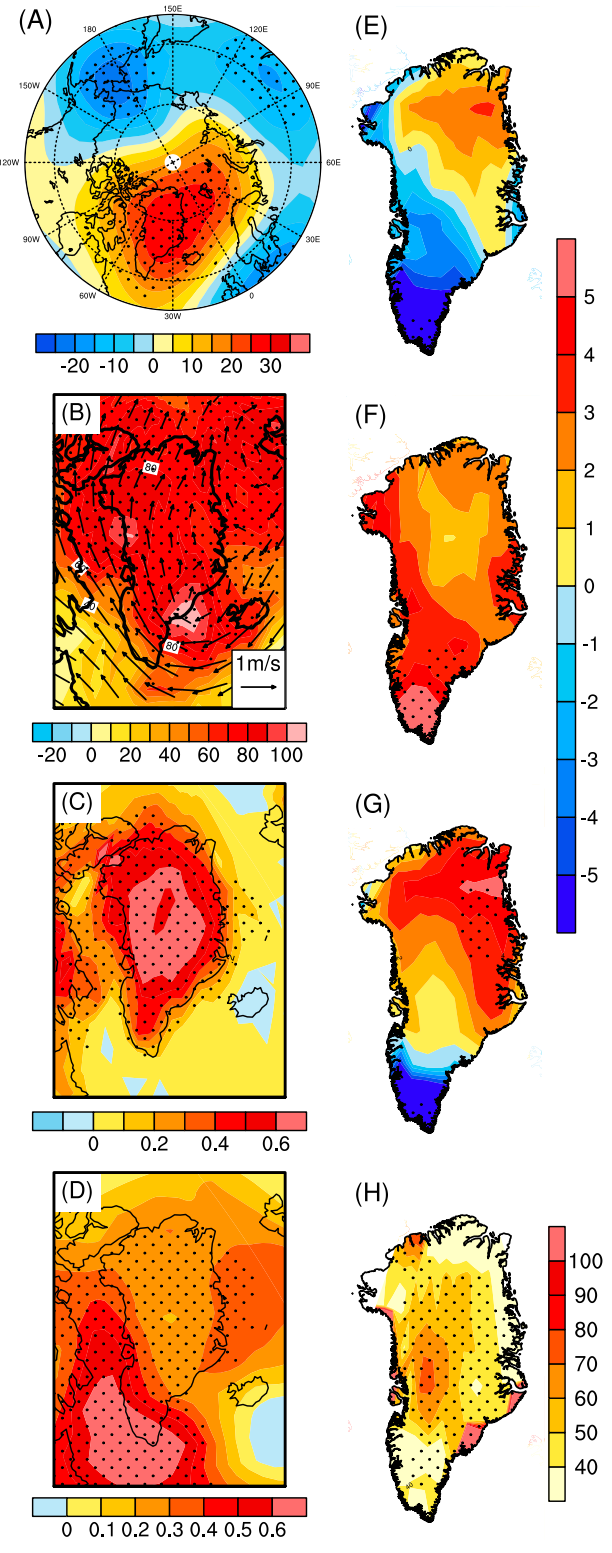

FIG. 11. Simulated summer atmospheric anomalies over Greenland in response to the reduction of summer Arctic sea ice (differences between the low and climatological sea ice simulations). (a)–(d) As in Fig. 2a,c,e,g and (e)–(h) as in Fig. 2i,k,m,o. Grid points that are statistically significant (>95% confidence level) are marked by black dots.

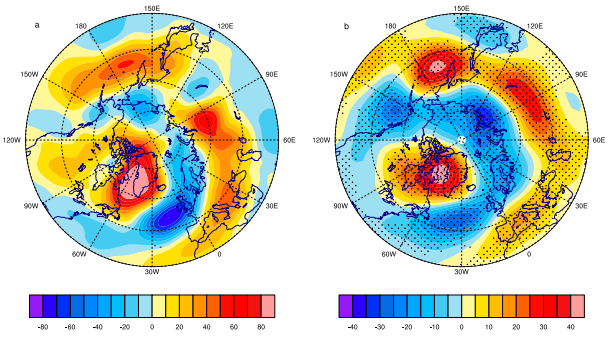

FIG. 12. The 500-hPa geopotential height anomalies in summer 2012. (a) ERA-Interim (relative to the climatology of 1982–2001) and (b) difference in simulated response to the observed sea ice concentration in summer 2012 and climatological sea ice concentration. Grid points that are statistically significant (>95% confidence level) are marked by black dots.

MODEL SIMULATIONS OF THE 2012 GREENLAND MELT EVENT

To further address the possibility that the atmospheric circulation over Greenland in a specific summer may result primarily from natural variability in the initial atmospheric state, we perform two additional sets of model ensemble experiments focused on the extreme surface melt of summer 2012, which was associated with an unusually persistent blocking circulation over Greenland (as indicated by the GMSE and GBI indices in Fig. 1). In one simulation the climatological sea ice concentration is prescribed, and the observed sea ice concentration during summer 2012 is used in the other. Both simulations are initialized with the observed atmospheric state on 1 June 2012 (see section 2 for details). We compare differences in simulated 500-hPa fields to observed 2012 anomalies based on ERA-Interim values. In summer 2012, the observed large-scale anomalies at 500 hPa featured a strong positive GPH over Greenland, which was accompanied by negative heights in an arc along the seas north of Eurasia (Fig. 12a). The strong similarity of patterns in the comparison between simulations to the observed anomalies (Fig. 12b vs Fig. 12a) suggests that differing sea ice conditions, and not the initial atmospheric state, is the primary driver of the positive GPH anomalies over Greenland in summer 2012. The magnitude of the simulated response is relatively weaker than that of the observed anomalies, but this is expected owing to averaging of the model ensemble members. This simulation of the extreme Greenland surface melt event in summer 2012 further supports the role of Arctic sea ice loss in forcing the persistent blocking high over Greenland, given that both simulations are started from the same observed initial atmospheric condition in a specific summer.

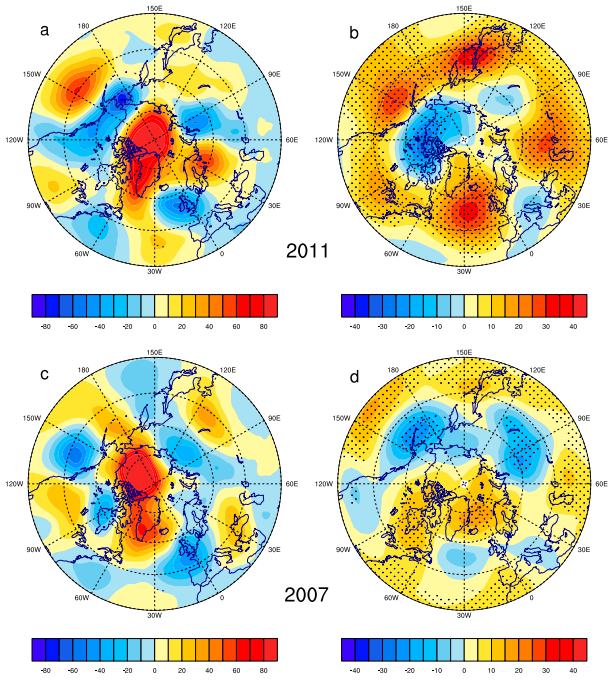

FIG. 13. As in Fig. 12, but for summer (top) 2011 and (bottom) 2007.

To confirm the robustness of the summer 2012 case, following the same procedure used to simulate conditions for the summer 2012 experiments, we conduct additional sets of numerical experiments for summer 2011 (second-lowest summer ASIE; Fig. 1a) and 2007 (third-lowest summer ASIE; Fig. 1a). The ensemble-mean difference between observed sea ice loss in 2011 and 2007 and climatology simulations also shows positive height anomalies over Greenland (Fig. 13), consistent with the results for the 2012 simulation.

Figure 14a shows observed summer surface temperature trends over Greenland during 1979–2013. Greenland is dominated by a strong warming, approximately 2°–3°C for the past 35 yr. We also calculate the fraction of summer surface temperature trend congruent with the summer ASIE by regressing surface temperature anomalies on the ASIE (Fig. 14b). The signature of Arctic sea ice decline is strongly associated with both the pattern and amplitude of the observed trends in surface temperature over Greenland. This is also true for extreme heat events (cf. Figs. 14d and 14e). Nearly all of the warming (as well as changes in extreme heat events) is linearly congruent with Arctic sea ice decline.

5. Discussion and conclusions

In this study we present multiple lines of evidence, based on both analyses of observational (reanalysis) data and independent confirmation from atmospheric

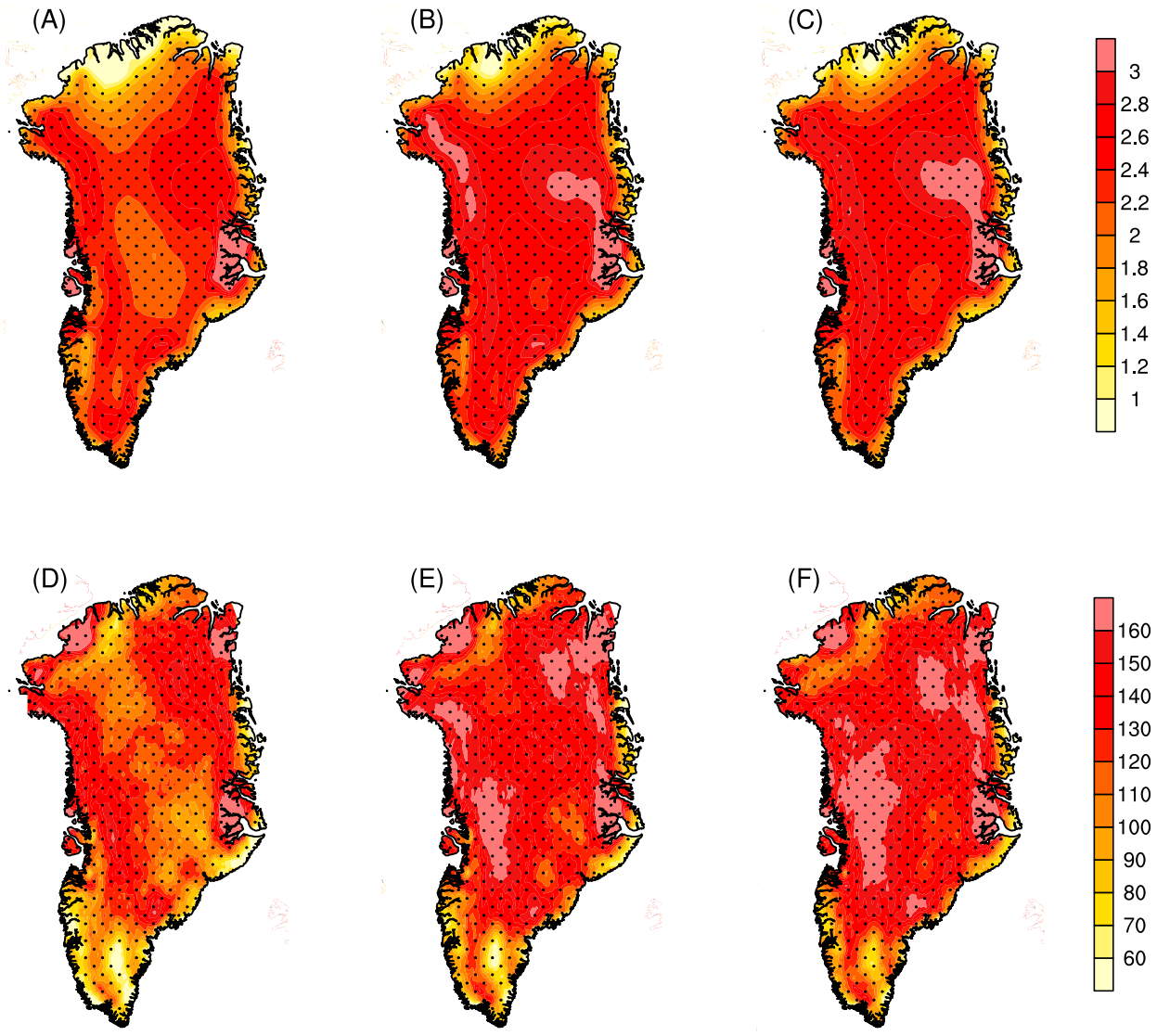

FIG. 14. Temperature trends [°C (35 yr)$^{-1}$] over Greenland. (a) Linear trend of summer-mean surface temperature. Components of the trend that are linearly congruent with the summer (b) ASIE and (c) GSME. (d)–(f) As in (a)–(c), but for the summer extreme heat events. Note that the sign of ASIE is reversed.

model simulations, that reveal a linkage between recent Arctic sea ice loss and Greenland surface melt. Our results suggest that dynamic and thermodynamic signatures of the atmospheric response to sea ice loss have contributed to the recent increase in surface melting of Greenland's ice sheet.

It is well known that natural variability is large in the high-latitude atmospheric circulation, presenting a challenge to detecting signals of change. As shown in Fig. 1a, the summer NAO (the dominant mode of atmospheric variability at high latitudes in the North Atlantic) has exhibited a pronounced decreasing trend since the mid-1990s, which may be suspected as a factor in controlling the covariability between the summer ASIE and GSME. The correlations between the summer NAO and the ASIE (with trend) and with the GSME are 0.54 and −0.48, respectively, which are much smaller than that between the summer ASIE and GSME (−0.91). After removing the linear trend, the correlations are reduced to 0.41 and −0.25, respectively, which are also much smaller than that between the detrended summer ASIE and GSME (−0.61). This suggests a stronger covariability between the summer ASIE and GSME than with either of these and the NAO.

To isolate the linkage between the summer ASIE and GSME in light of the recent change in the summer NAO

index, we use linear regression models to calculate the ASIE and GSME using the NAO as predictor. The regression models are $Y'_{\mathrm{ASIE}} = A_1X_{\mathrm{NAO}} + B_1$ and $Y'_{\mathrm{GSME}} = A_2X_{\mathrm{NAO}} + B_2$, where X_{NAO} is the standardized NAO index, and Y'_{ASIE} and Y'_{GSME} are the ASIE and GSME influenced by the NAO. We then calculate the residual time series; that is, 1) the difference between the observed ASIE and the ASIE influenced by the NAO (Y'_{ASIE}) and 2) the difference between the observed GSME and the GSME influenced by the NAO (Y'_{GSME}). Thus, the residuals are independent of the NAO because the impacts of the NAO are removed. The correlations between the two residual time series are −0.89 (with trend) and −0.71 (without trend), indicating a significant relationship between the summer ASIE and GSME that is independent of the summer NAO.

Projections from phase 5 of the Coupled Model Intercomparison Project show a further decline of Arctic sea ice, driven by continued anthropogenic emission of greenhouse gases (e.g., Wang and Overland 2012; Liu et al. 2013). The results presented here implicate a mechanism linking sea ice loss to increased surface heat fluxes over Greenland, which favor positive GPH anomalies over Greenland and the central Arctic Ocean, increased blocking events, and warming throughout the region. This linkage establishes a positive feedback between the decline in Arctic sea ice and expanding surface melt of the Greenland ice sheet. Thus, as sea ice continues to decline in the future, further melt of Greenland's ice cap should also transpire, contributing to accelerating global sea level rise. The additional freshwater input from the Greenland Sea is also expected to suppress the formation of the North Atlantic Deep Water, an important driver of the global ocean's thermohaline circulation. The atmospheric response to sea ice loss identified in the study also suggests that weather patterns in the North Atlantic region and Europe will become more persistent, possibly leading to an increased frequency of extreme weather events in summer. It is imperative for climate models to realistically simulate these relationships so that evolving atmospheric circulation patterns and the mass balance of the Greenland ice sheet can be captured accurately as greenhouse gas emissions continue unabated.

Acknowledgments. J. L. is supported by the Climate Observation and Earth System Science Divisions, Climate Program Office, NOAA, U.S. Department of Commerce (NA15OAR4310163 and NA14OAR4310216). J. F. is supported by the NSF ARCSS (1304097), M. S. is supported by the NSFC (41305097), and T. M. is supported by NASA IDS Grant NNX14AD98G. We thank anonymous reviewers for their time and feedback.

REFERENCES

Abdalati, W., and K. Steffen, 2001: Greenland ice sheet melt extent: 1979–1999. *J. Geophys. Res.*, **106**, 33 983–33 988, doi:10.1029/2001JD900181.

Alley, R., P. Clark, P. Huyberchts, and I. Joughin, 2005: Ice-sheet and sea level changes. *Science*, **310**, 456–460, doi:10.1126/science.1114613.

Bennartz, R., M. Shupe, D. Turner, V. Walden, K. Steffen, C. Cox, M. Kulie, N. Miller, and C. Pettersen, 2013: July 2012 Greenland melt extent enhanced by low-level liquid clouds. *Nature*, **496**, 83–86, doi:10.1038/nature12002.

Box, J., X. Fettweis, J. Stroeve, M. Tedesco, D. Hall, and K. Steffen, 2012: Greenland ice sheet albedo feedback: Thermodynamics and atmospheric drivers. *Cryosphere*, **6**, 821–839, doi:10.5194/tc-6-821-2012.

Cohen, J., and Coauthors, 2014: Recent Arctic amplification and extreme mid-latitude weather. *Nat. Geosci.*, **7**, 627–637, doi:10.1038/ngeo2234.

Collins, W., and Coauthors, 2006: The formulation and atmospheric simulation of the Community Atmosphere Model Version 3 (CAM3). *J. Climate*, **19**, 2144–2161, doi:10.1175/JCLI3760.1.

Comiso, J., 2000: Bootstrap sea ice concentrations from Nimbus-7 SMMR and DMSP SSM/I-SSMIS, version 2. National Snow and Ice Data Center, accessed February 2015, doi:10.5067/J6JQLS9EJ5HU.

Coumou, D., J. Lehmann, and J. Beckmann, 2015: The weakening summer circulation in the Northern Hemisphere mid-latitudes. *Science*, **348**, 324–327, doi:10.1126/science.1261768.

Cuffey, K., and S. Marshall, 2000: Substantial contribution to sea-level rise during the last interglacial from the Greenland ice sheet. *Nature*, **404**, 591–594, doi:10.1038/35007053.

Dee, D., and Coauthors, 2011: The ERA-Interim reanalysis: Configuration and performance of the data assimilation system. *Quart. J. Roy. Meteor. Soc.*, **137**, 553–597, doi:10.1002/qj.828.

Ding, Q., J. Wallace, D. Battisti, E. Steig, A. Gallant, H. Kim, and L. Geng, 2014: Tropical forcing of the recent rapid Arctic warming in northeastern Canada and Greenland. *Nature*, **509**, 209–212, doi:10.1038/nature13260.

Dumont, M., and Coauthors, 2014: Contribution of light-absorbing impurities in snow to Greenland's darkening since 2009. *Nat. Geosci.*, **7**, 509–512, doi:10.1038/ngeo2180.

Enderlin, E., M. Howat, S. Jeong, M. Noh, J. van Angelen, and M. van den Broeke, 2014: An improved mass budget for the Greenland ice sheet. *Geophys. Res. Lett.*, **41**, 866–872, doi:10.1002/2013GL059010.

Fang, Z.-F., 2004: Statistical relationship between the Northern Hemisphere sea ice and atmospheric circulation during wintertime. *Observation, Theory and Modeling of Atmospheric Variability*, X. Zhu, Ed., World Scientific Series on Asia-Pacific Weather and Climate, Vol. 3, World Scientific, 131–141.

Fetterer, F., K. Knowles, W. Meier, and M. Savoie, 2002: Sea ice index, version 1. National Snow and Ice Data Center, accessed February 2015, doi:10.7265/N5QJ7F7W.

Fettweis, X., M. Tedesco, M. van den Broeke, and J. Ettema, 2011: Melting trends over the Greenland ice sheet (1958–2009) from spaceborne microwave data and regional climate models. *Cryosphere*, **5**, 359–375, doi:10.5194/tc-5-359-2011.

Francis, J., and S. Vavrus, 2012: Evidence linking Arctic amplification to extreme weather in mid-latitudes. *Geophys. Res. Lett.*, **39**, L06801, doi:10.1029/2012GL051000.

——, and ——, 2015: Evidence for a wavier jet stream in response to rapid Arctic warming. *Environ. Res. Lett.*, **10**, 014 005, doi:10.1088/1748-9326/10/1/014005.

Hakkinen, S., D. Hall, C. Shuman, D. Worthen, and N. DiGirolamo, 2014: Greenland ice sheet melt from MODIS and associated atmospheric variability. *Geophys. Res. Lett.*, **41**, 1600–1607, doi:10.1002/2013GL059185.

Hall, R., R. Erdélyi, E. Hanna, J. Jones, and A. Scaife, 2015: Drivers of North Atlantic polar front jet stream variability. *Int. J. Climatol.*, **35**, 1697–1720, doi:10.1002/joc.4121.

Hanna, E., J. Jones, J. Cappelen, S. Mernild, L. Wood, K. Steffen, and P. Huybrechts, 2013a: The influence of North Atlantic atmospheric and oceanic forcing effects on 1900–2010 Greenland climate and ice melt/runoff. *Int. J. Climatol.*, **33**, 862–880, doi:10.1002/joc.3475.

——, and Coauthors, 2013b: Ice-sheet mass balance and climate change. *Nature*, **498**, 51–59, doi:10.1038/nature12238.

——, X. Fettweis, S. Mernild, J. Cappelen, M. Ribergaard, C. Shuman, K. Steffen, L. Wood, and T. Mote, 2014: Atmospheric and oceanic climate forcing of the exceptional Greenland ice sheet surface melt in summer 2012. *Int. J. Climatol.*, **34**, 1022–1037, doi:10.1002/joc.3743.

——, T. Cropper, P. Jones, A. Scaife, and R. Allan, 2015: Recent seasonal asymmetric changes in the NAO (a marked summer decline and increased winter variability) and associated changes in the AO and Greenland blocking index. *Int. J. Climatol.*, **35**, 2540–2554, doi:10.1002/joc.4157.

Hu, A., G. Meehl, W. Han, and J. Yin, 2011: Effect of the potential melting of the Greenland ice sheet on the meridional overturning circulation and global climate in the future. *Deep-Sea Res. II*, **58**, 1914–1926, doi:10.1016/j.dsr2.2010.10.069.

Kapsch, M., R. Graversen, T. Economou, and M. Tjernström, 2014: The importance of spring atmospheric conditions for predictions of the Arctic summer sea ice extent. *Geophys. Res. Lett.*, **41**, 5288–5296, doi:10.1002/2014GL060826.

Liu, J., J. Curry, H. Wang, M. Song, and R. Horton, 2012: Impact of declining Arctic sea ice on winter snowfall. *Proc. Natl. Acad. Sci. USA*, **109**, 4074–4079, doi:10.1073/pnas.1114910109.

——, M. Song, R. Horton, and Y. Hu, 2013: Reducing spread in climate model projections of a September ice-free Arctic. *Proc. Natl. Acad. Sci. USA*, **110**, 12 571–12 576, doi:10.1073/pnas.1219716110.

Markus, T., J. C. Stroeve, and J. Miller, 2009: Recent changes in Arctic sea ice melt onset, freezeup, and melt season length. *J. Geophys. Res.*, **114**, C12024, doi:10.1029/2009JC005436.

Meier, M., M. Dyurgerov, U. Rick, S. O'Neel, W. Pfeffer, R. Anderson, S. Anderson, and A. Glazovsky, 2007: Glaciers dominate eustatic sea-level rise in the 21st century. *Science*, **317**, 1064–1067, doi:10.1126/science.1143906.

Mernild, S., T. Mote, and G. Liston, 2011: Greenland ice sheet surface melt extent and trends: 1960–2010. *J. Glaciol.*, **57**, 621–628, doi:10.3189/002214311797409712.

Mote, T., 2007: Greenland surface melt trends 1973–2007: Evidence of a large increase in 2007. *Geophys. Res. Lett.*, **34**, L22507, doi:10.1029/2007GL031976.

——, M. Anderson, K. Kuivinen, and C. Rowe, 1993: Passive microwave-derived spatial and temporal variations of summer melt on the Greenland ice sheet. *Ann. Glaciol.*, **17**, 233–238.

Nghiem, S., and Coauthors, 2012: The extreme melt across the Greenland ice sheet in 2012. *Geophys. Res. Lett.*, **39**, L20502, doi:10.1029/2012GL053611.

Overland, J., J. A. Francis, R. Hall, E. Hanna, S.-J. Kim, and T. Vihma, 2015: The melting Arctic and midlatitude weather patterns: Are they connected? *J. Climate*, **28**, 7917–7932, doi:10.1175/JCLI-D-14-00822.1.

Pithan, F., and T. Mauritsen, 2014: Arctic amplification dominated by temperature feedbacks in contemporary climate models. *Nat. Geosci.*, **7**, 181–184, doi:10.1038/ngeo2071.

Rayner, N., D. Parker, E. Horton, C. Folland, L. Alexander, D. Rowell, E. Kent, and A. Kaplan, 2003: Global analyses of sea surface temperature, sea ice, and night marine air temperature since the late nineteenth century. *J. Geophys. Res.*, **108**, 4407, doi:10.1029/2002JD002670.

Rennermalm, A., L. Smith, J. Stroeve, and V. Chu, 2009: Does sea ice influence Greenland ice sheet surface-melt? *Environ. Res. Lett.*, **4**, 024 011, doi:10.1088/1748-9326/4/2/024011.

Rignot, E., J. Box, E. Burgess, and E. Hanna, 2008: Mass balance of the Greenland ice sheet from 1958 to 2007. *Geophys. Res. Lett.*, **35**, L20502, doi:10.1029/2008GL035417.

Rossow, W., and R. Schiffer, 1999: Advances in understanding clouds from ISCCP. *Bull. Amer. Meteor. Soc.*, **80**, 2261–2288, doi:10.1175/1520-0477(1999)080<2261:AIUCFI>2.0.CO;2.

Screen, J., and I. Simmonds, 2010: The central role of diminishing sea ice in recent Arctic temperature amplification. *Nature*, **464**, 1334–1337, doi:10.1038/nature09051.

——, C. Deser, I. Simmonds, and R. Tomas, 2014: Atmospheric impacts of Arctic sea-ice loss, 1979–2009: Separating forced change from atmospheric internal variability. *Climate Dyn.*, **43**, 333–344, doi:10.1007/s00382-013-1830-9.

Serreze, M., and R. Barry, 2011: Processes and impacts of Arctic amplification: A research synthesis. *Global Planet. Change*, **77**, 85–96, doi:10.1016/j.gloplacha.2011.03.004.

Shannon, S., and Coauthors, 2013: Enhanced basal lubrication and the contribution of the Greenland ice sheet to future sea-level rise. *Proc. Natl. Acad. Sci. USA*, **110**, 14 156–14 161, doi:10.1073/pnas.1212647110.

Shepherd, A., and Coauthors, 2012: A reconciled estimate of ice-sheet mass balance. *Science*, **338**, 1183–1189, doi:10.1126/science.1228102.

Stackhouse, P., S. Gupta, S. Cox, J. Mikovitz, T. Zhang, and L. Hinkelman, 2011: The NASA/GEWEX surface radiation budget release 3.0: 24.5-year dataset. *GEWEX News*, No. 21, GEWEX Project Office, Silver Spring, MD, 10–12.

Sundal, A., A. Shepherd, P. Nienow, E. Hanna, S. Palmer, and P. Hubrechts, 2011: Melt-induced speed-up of Greenland ice sheet offset by efficient subglacial drainage. *Nature*, **469**, 521–524, doi:10.1038/nature09740.

Tedesco, M., 2007: Snowmelt detection over the Greenland ice sheet from SSM/I brightness temperature daily variations. *Geophys. Res. Lett.*, **34**, L02504, doi:10.1029/2006GL028466.

——, X. Fettweis, M. van den Broeke, R. van de Wal, C. Smeets, W. van de Berg, M. Serreze, and J. Box, 2011: The role of albedo and accumulation in the 2010 melting record in Greenland. *Environ. Res. Lett.*, **6**, 014 005, doi:10.1088/1748-9326/6/1/014005.

——, ——, T. Mote, J. Wahr, P. Alexander, J. Box, and B. Wouters, 2013: Evidence and analysis of 2012 Greenland records from spaceborne observations, a regional climate model and reanalysis data. *Cryosphere*, **7**, 615–630, doi:10.5194/tc-7-615-2013.

Thompson, D., and J. Wallace, 2001: Regional climate impacts of the Northern Hemisphere annular mode. *Science*, **293**, 85–89, doi:10.1126/science.1058958.

Walsh, J., 2014: Intensified warming of the Arctic: Causes and impacts on middle latitudes. *Global Planet. Change*, **117**, 52–63, doi:10.1016/j.gloplacha.2014.03.003.

Wang, M., and J. Overland, 2012: Sea ice free summer Arctic within 30 years: An update from CMIP5 models. *Geophys. Res. Lett.*, **39**, L18501, doi:10.1029/2012GL052868.

Zwally, J., W. Abdalati, T. Herring, K. Larson, J. Saba, and K. Steffen, 2002: Surface melt-induced acceleration of Greenland ice-sheet flow. *Science*, **297**, 218–222, doi:10.1126/science.1072708.